VOL NUMBER 904/ISSUES 1–3 30 JUNE 2009 ISSN 0166-1280
Vol. 904 is complete in one issue

ELSEVIER

JOURNAL OF MOLECULAR STRUCTURE

THEOCHEM

Theory and Modelling in Chemistry

CLIFFORD DYKSTRA, AJIT J. THAKKAR and MANUEL YÁÑEZ

www.elsevier.com/locate/theochem

Journal of Molecular Structure: THEOCHEM 904 (2009) 28–34

Contents lists available at ScienceDirect

Journal of Molecular Structure: THEOCHEM

journal homepage: www.elsevier.com/locate/theochem

Circulene covered fullerenes

Mircea V. Diudea [a,*], Aniela E. Vizitiu [a], Titus Beu [a], Attila Bende [b], Csaba L. Nagy [a], Dušanka Janežič [c]

[a] "Babes-Bolyai" University, Arany Janos 11, 400028 Cluj-Napoca, Romania
[b] National Institute for R&D of Isotopic and Molecular Technologies, Donath Str. 65-103, 400293 Cluj-Napoca, Romania
[c] National Institute of Chemistry, Ljubljana, Slovenia

ARTICLE INFO

Article history:
Received 21 November 2008
Received in revised form 16 February 2009
Accepted 23 February 2009
Available online 28 February 2009

Keywords:
Fullerenes
DFT
Electronic structure
Aromaticity

ABSTRACT

Covering fullerenes by circulene bowl-shaped units can be performed by using operations on maps, geometrical–topological transformations of a polyhedral tessellation.

Quantum chemical calculations and the HOMA geometric index of aromaticity are used to evaluate the stability of the novel designed fullerenes. Electronic structure and IR spectra are obtained by DFT calculations. The HOMO orbitals localized on circulenic faces in conjunction with more delocalized LUMO orbitals suggest possible Jahn–Teller distortions of the structures. Similarly tessellated classical or non-classical fullerenes show similar IR spectral properties.

The variation in aromaticity of one and the same circulene/flower, function of the molecular context, is explained by considering the strain of cages as an important destabilizing factor.

1. Introduction

Since the discovery [1] of C_{60} "Buckminsterfullerene" and its synthesis in macroscopic quantities [2] by electric arc discharge, a multitude of studies were devoted to the understanding of the mechanism of synthesis and relation between the polyhedral structure and fullerene stability [3–7]. The synthesis by "wet chemistry" of fullerenes with controlled tessellation was another goal (not yet reached!) of researchers in this area. Recall in this respect the synthesis of $C_{20}H_{20}$-hydrocarbon [8]. It is hoped that the "artificial" synthesis of fullerenes with desired tessellation may be achieved *via* circulene units, or flowers Fw, $[n_{core}:(m_{petal})_n]$. Several circulene (*i.e.*, flower) units reported to date [9–11], *e.g.*, coronene [6:66] and sumanene [6:(5,6)] were referred as being fullerene substructures.

The idea that aromaticity and stability of fullerenes may be increased when they are tessellated by disjoint flowers originates in the classical texts of Clar [12,13], who postulated *disjoint benzenoid rings* (those rings having six π-electrons localized in double–single alternating bonds and separated from adjacent rings by formal single bonds), as a criterion for the full aromatic conjugation. Molecular structures, showing such fully *resonant sextets* are expected, according to valence bond theory [14–16], to be extremely stable.

A set of disjoint faces, built up over all atoms of the molecule, is called a perfect Clar (PC) structure. In fullerenes, a PC structure includes, however, all the pentagonal faces, which are usually assigned as empty π-electron faces, and also, some hexagonal faces. A Kekulé valence structure is a set of pairwise disjoint bonds, defined over all atoms of the molecule. It has been demonstrated that fullerenes show a PC structure if and only if they have a Fries structure, *i.e.*, a Kekulé structure having the maximum possible (v/3) number of benzenoid faces [17,18]. The PC structure consists of full π-electron, disjoint hexagons, as previously suggested by Clar, only in polyhex structures (*e.g.*, polyhex tori), where the assignment empty/full can be interchanged at two adjacent hexagons. Thus, the PC structure and its associate Fries structure will ensure the total resonance or conjugation of the molecule.

Using the HF/GAP ratio (*i.e.*, the ratio of the heat of formation to the HOMO–LUMO gap), as a rough measure of fullerene stability, we found, in several sets of isomeric fullerenes [19] that the fullerenes tessellated by disjoint flowers are the most stable, as shown below.

The two most stable isomers of the series C_{40} show D_2 and D_{5d}, symmetry. The isomer 39-D_{5d} is described in the Atlas of Fullerenes [20] as a "lens" of two corannulenic flowers [5:65], whose largest HOMO–LUMO gap (6.259 eV) is supposed to originate in its disjoint flower DFw structure. In spite of the fact that the isomer 38-D_2 shows a slightly lower HF/atom (a measure of thermodynamic stability of a molecule) and lower strain energy, its gap is significantly lower, implying a lower kinetic stability of this molecule in comparison to the isomer 39-D_{5d}, whose HF/GAP ratio is the lowest recorded in this series.

In the C_{42} fullerene series, the lowest values of the strain and HF/Gap ratios are shown by the isomer 45-D_3. This structure is tiled by two sumanenic [6:(5,6)] disjoint flowers, sumanene being a recently synthesized molecule [5,6]. In the C_{48} fullerene series, the isomer of D_{6d} symmetry, tessellated by two coronenic [6:6_6]

* Corresponding author.
E-mail address: diudea@chem.ubbcluj.ro (M.V. Diudea).

0166-1280/$ - see front matter © 2009 Elsevier B.V. All rights reserved.
doi:10.1016/j.theochem.2009.02.024

disjoint flowers, shows the largest gap (5.988 eV). Its strain energy, calculated in terms of POAV1 approach [21,22], is however larger in comparison to that of the energetically better ranked isomers.

Similar conclusions can be drawn for the C_{84} series, where the isomer 20-T_d shows the largest gap (6.233 eV) and strain which is the third highest in the series of IPR fullerenes of 84 atoms. The HF/GAP ratio (8.211 eV) is the lowest in this series, even lower than that shown by C_{60} (8.890 eV), but the isomer 20-T_d is not among the nine C_{84} isomers (#4, 5, 11, 14, 16, 19, 22, 23 and 24) that have so far been isolated [23].

The isolated isomer #24, shows considerably reduced strain and is only the thirteenth highest strain in the series. It also exhibits the third lowest HF/GAP ratio and is the third lowest in energy. The most stable isomer in this series, #23, is ranked the lowest in energy, the third lowest in strain and has the fourth lowest HF/GAP ratio. In terms of the HOMA index of aromaticity, #5 is the most aromatic structure in the series and #23 is the second most aromatic structure. The above data (related to the PM3 level of theory) argue in favor of an important role for the HOMO–LUMO gap in stabilizing the molecule, and against the net strain, which acts in the opposite direction.

Tessellation of a sphere with various circulene flowers can be performed *in silico* with the aid of operations on maps. In this respect, there are the well-known Leapfrog/Tripling $Le_{1,1}$, Chamfering/Quadrupling $Q_{2,0}$ and Capra/Septupling $Ca_{2,1}$ operations. A number of recent papers described these procedures [24–27]. Of these, Le is the only operation providing PC transforms, which can be embedded in surfaces of any genera. Patterns larger than benzene, *e.g.* naphthalene or azulene, have also been considered with respect to the Clar theory. By extension [27,28], flowers, or circulene supra-faces could play an important role in the stability of fullerenes.

A *joint flower* JFw pattern may form either a Platonic, having a single type of flower), *e.g.*, [5:6_5], [6:6_6] or [7:6_7] (in case of open structures), or an Archimedean, with two types of flowers, *e.g.*, [5:6_5]&[6:6_6], supra-covering. The vertex degree of the net is, in the most cases, 3. The case of Platonic [5:6_5]JFw covering is unique and can be achieved by operation: $Ca_{2,1}(D) = C_{140}$; D = dodecahedron.

A *disjoint flower* DFw structure is a disjoint set of flowers, covering all the vertices in the molecular graph. Some sequences of operations (*e.g.*, Le and Q; $Q_{4,0,c}$ and Tr_s) or the generalized $Le_{2,2}$ operation can provide a DFw covering and such a transform is necessarily associated with a PC structure, but the reciprocal need not always be true. The cage C_{240} is a Platonic DFw covering (Fig. 1a). Any covering flower has a co-Fw; in the top of figures, the π-electron population (*i.e.*, numerical Kekulé count [29]) is often given (Fig. 1b).

The supra-organized flower units are expected to contribute to the stability of the whole molecule [27,28] and semi-empirical calculations with the PM3 Hamiltonian provided a partial proof of this expectation [28].

Coronene itself [6:6_6]Fw is not a totally resonant hydrocarbon [29], because any Kekulé structure leaves some carbon atoms outside sextet rings. However, it was suggested by Clar et al. [30] that, if the three sextets of coronene can migrate into the neighboring rings, this fact will enhance the aromaticity of coronene, in comparison to other polycyclic hydrocarbons such as naphthalene and anthracene [31].

Counter circulation of "rim and hub" currents is a characteristic of the circulenes [n]Fw, as shown by the ipsocentric [32] continuous transformation of origin of current density (CTOCD) calculations [33,34]. This is one reason for the need of a disjoint DFw structure. Note that the ring-current calculations [35] do not support the Clar's hypothesis about the super-aromaticity of coronene.

A comparison of several fullerene isomers of 240 atoms, designed by various sequences of map operations, is presented in Table 1. The plot HOMA vs. HF/GAP (Fig. 2) shows that the variance of aromaticity is almost completely accounted for by the HF/GAP ratio.

The article is structured as follows. Section 2 presents the methods used for the design of structures, the evaluation of energy and aromaticity characterization and the fullerenes thus designed. The data are discussed in Section 3 and finally the conclusions and references are presented.

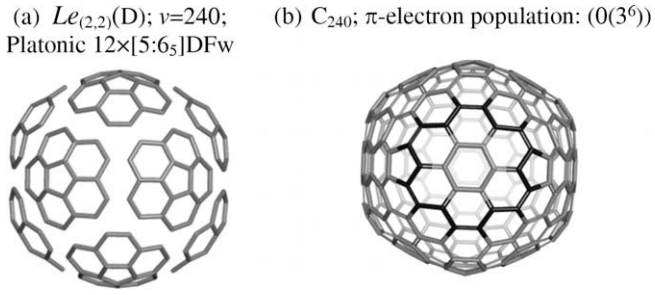

Fig. 1. C_{240}: (a) a corannule DFw; (b) a coronene co-Fw.

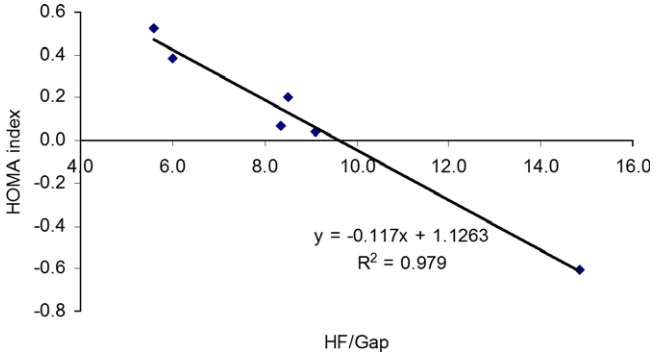

Fig. 2. Plot of HF/Gap vs. HOMA index in the series of 240 cages in Table 1.

Table 1
Data for some (closed π-shell) cages built upon 240 atoms: symmetry Sym; heat of formation, HF/atom (PM3) (kcal/mol); HOMO–LUMO Gap (eV); HF/GAP (×100; eV); strain energy SE/atom (kcal/mol; POAV1); HOMA index of aromaticity. The bold letters in the name of cages refer to: D (dodecahedron), C (cube) and O (octahedron).

	Cage	Sym.	HF/atom (kcal/mol)	GAP (eV)	HF/GAP	SE/atom	HOMA	Operation sequence
1	240**D**-12	O_h	6.584	5.113	5.587	2.506	0.524	$Le_{(2,2)} = Le(Q(M))$
2	240**O**-40RO	O_h	7.283	5.273	5.993	2.107	0.386	$RO(Tr_s(Q(S_2(M))))$
3	240**O**-40	O_h	4.783	4.783	8.502	2.357	0.205	$Tr_s(Q(S_2(M)))$
4	240**C**/**O**-30	O	10.666	5.530	8.371	3.002	0.068	$Le(P_5(Me(M)))$
5	240**C**-30RO	O_h	12.960	6.175	9.107	4.285	0.044	$RO(Tr_s(Q(S_2(M))))$
6	240**C**-30	O	15.918	4.656	14.836	2.719	-0.602	$Tr_s(Ca_{(3,,2c)}(M))$

2. Methods and results

2.1. Structure design

We designed the cages shown in Fig. 3 by using sequences of operations on maps [27,36], as implemented in our software Cage-Versatile [37]. We considered the small classical fullerenes (#1 to #3), numbered as in the Atlas of Fullerenes [20], some non-classical fullerenes (#4 to #8), with faces other than pentagons and hexagons, and the Buckminsterfullerene C_{60}, C_{84} (Fig. 4a), and C_{96} (Fig. 4b).

The sequence Le($S_2(T)$) provides a disjoint sumanenic [n:(5,6)$_{n/2}$]DFw pattern, in a Platonic covering [27]. The co-Fw forms an Archimedean covering of coronenic [n:6$_n$]Fw and pentylenic [p:(0,5))$_{p/2}$]Fw patterns. The tripentylene [6:(0,5)$_3$]Fw can be viewed as an analog of the triphenylene [6:(0,6)$_3$]Fw. Fig. 4a illustrates the above covering for the transform of tetrahedron (#9) 84T-21; (84:20-T_d) [20], of tetrahedral symmetry and Platonic covering: 4×[6:(5,6)$_3$]DFw; 4×[6:6$_6$]co-JFw; 4×[(6:(0,5)$_3$]co-JFw; HOMA=0.251 (classified as the highest aromatic among structures generated by Le($S_2(T)$) sequence).

Another sequence, Tr$_s$(Ca$_f$(Q(M))) (where Q is the Quadrupling operation, Ca$_f$ represents the Capra operation performed in such a way that the original faces of M remain untransformed while Tr$_s$ is the truncation of selected vertices), leads to a Platonic disjoint flower pattern [n:(7(5d))$_n$]DFw. This is a chiral covering, by virtue of *Ca*, and shows a co-flower co-Fw of sumanenic [n:(5,6)$_{n/2}$]Fw type [27].

Next, the Stone–Wales [38] SW rotation of the spokes of the n-gonal hub of [n:(7(5d))$_n$]Fw results in a Platonic covering by disjoint corazenic [n:(5,7)$_{n/2}$]Fw patterns. The rotation also changes the sumanenic co-Fw to the corazenic co-Fw, so that both Fw and co-Fw are corazenic and both are disjoint. The representative structure of this sequence of operations is (#10) 96T-24RO (Fig. 4b), which has tetrahedral symmetry and Platonic covering: 4×[6:(5,7)$_3$]DFw; 4×[6:(5,7)$_3$]co-DFw; HOMA = 0.017, classified as non-aromatic by this geometric criterion.

Alternatively, a Platonic anti-aromatic disjoint pattern by (12) pentalenes (*i.e.*, abutting pentagons) can be evidenced. The tessellation by disjoint pentalenes represents a generalized [27] perfect Clar structure, in the sense that the faces composing the 2-factor represent the pentalenic contours.

If the Buckminsterfullerene C_{60} (60:1-I_h) (#11), of icosahedral symmetry and sumanenic covering, is taken as a reference structure, then 4×[6:(5,6)$_3$]JFw; 4 × R$_6$ co-Fw; HOMA = 0.169, and it may be classified as low aromatic. The large value of the HOMO–LUMO gap ensures a lower value of the HF/GAP ratio, which can be taken as a rough measure of stability of a molecular structure. The relatively higher strain shown by C_{60} is, by symmetry, equally distributed over all its atoms, which are all equivalent, so that it

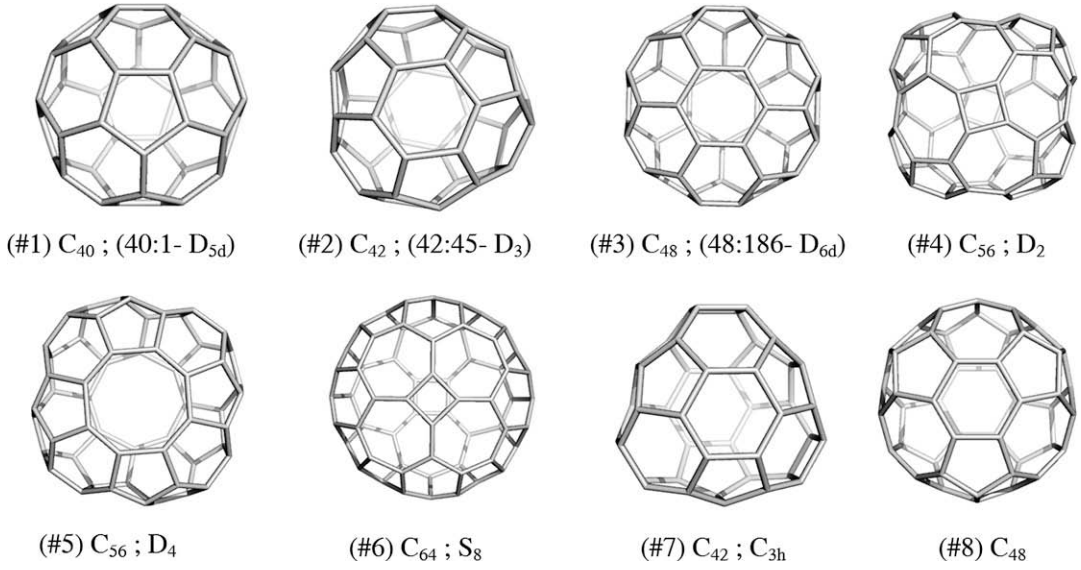

Fig. 3. Small cages with disjoint flower DFw tessellation.

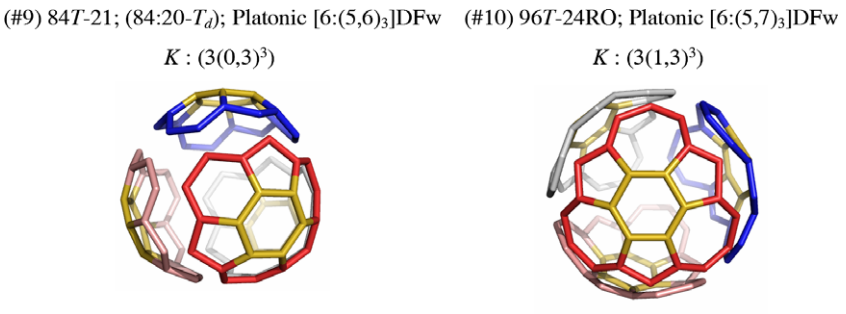

Fig. 4. Platonic disjoint sumanenic [6:(5,6))$_3$]DFw (a) and corazenic [6:(5,7)$_3$]DFw coverings. The numerical Kekulé count K for the π-electron local distribution in each case is given.

Table 2
PM3 data.

#	Structure (main flower)	Sym.	HF/atom (kcal/mol)	GAP (eV)	HF/GAP (×100)	SE/atom (kcal/mol)
1	C_{40}: 2[5:6_5]	D_{5d}	20.628	6.258	14.302	13.066
2	C_{42}: 2[6:(5,6)$_3$]	D_3	19.676	5.908	14.449	12.329
3	C_{48}: 2[6:6_6]	D_{6d}	21.972	5.988	15.923	12.612
4	C_{56}: 2[4:(7(5c))$_4$]	D_4	22.818	4.715	21.000	10.843
5	C_{56}: 2[8:(5,6)$_4$]	D_4	22.129	5.116	18.767	11.212
6	C_{64}: 2[4:(7(5d))4]	D_{4d}	24.071	4.945	21.121	10.140
7	C_{42}: 2[6:(5,6)$_3$]	D_{3h}	20.534	6.668	13.346	12.699
8	C_{48}: 2[6:(5,7)$_3$]	D_{3d}	22.238	4.932	19.563	11.572
9	C_{84}: 4[6:(5,6)$_3$]	T_d	11.795	6.234	8.213	6.334
10	C_{96}: 4[6:(5,7)$_3$]	T_h	13.869	4.78	12.59	5.348
11	C_{60}: 4[6:(5,6)$_3$]	I_h	13.512	6.593	8.890	8.257

does not destabilize the molecule excessively. The geometric criterion of aromaticity HOMA allows classification of C_{60} as a low aromatic molecule, a result already known [39–43]. The HOMA calculations were performed by a routine implemented in our JSCHEM software package [44].

For corazene/isocoronene [6:(5,7)$_3$], Fowler et al. [35] have recently predicted, in the ipsocentric [32] description, a single, unopposed, intense diatropic perimeter current arising from its four π-HOMO electrons; they qualified isocoronene as *super-aromatic*, by the magnetic criterion. By the energetic criterion, the coronene is, however, more aromatic and more stable.

2.2. PM3 data

Calculations at the PM3 level of theory have been performed for the above 11 structures, the results being listed in Table 2. The most stable structures are those showing the lowest HF/GAP ratio (entries 9–11).

2.3. DFT calculations

In the DFT calculations, we have used the GAUSSIAN 03 package [45] for performance of all-electron geometrical structure optimization and subsequent IR-spectrum calculations for the fullerene cages under consideration.

Both the basis sets 6-31g and 6-31g(d) proved to yield reliable and comparable results with reasonable computation costs. However, use of the polarized basis set 6-31g(d) turns out to be too time-consuming for the IR-spectrum calculations so that it was not used in our calculations.

Table 3 shows the electronic structures provided by our DFT calculations. Simulated IR spectra are shown in Fig. 5. The most intense IR-active vibrational modes of the fullerenes under study are presented in Fig. 6.

Table 3
DFT electronic structure results based on the PBE–PBE functional and the 6-31g basis set.

#	Structure	Total energy/atom (a.u.)	Sym.	HOMO (a.u.)	HOMO–LUMO GAP (a.u.)
1	C_{40}: 2[5:6_5]	−38.051	D_{5d}	−0.195	0.037
2	C_{42}: 2[6:(5,6)$_3$]	−38.052	D_3	−0.195	0.033
3	C_{48}: 2[6:6_6]	−38.048	D_{6d}	−0.190	0.028
4	C_{56}: 2[4:(7(5c))$_4$]	−38.049	D_4	−0.161	0.024
5	C_{56}: 2[8:(5,6)$_4$]	−38.049	D_4	−0.176	0.017
9	C_{84}: 4[6:(5,6)$_3$]	−38.062	T_d	−0.199	0.060
10	C_{96}: 4[6:(5,7)$_3$]	−38.060	T_h	−0.1694	0.0012

3. Discussion

Several operations on maps enabled us to design some classical and non-classical fullerenes. A collection of such fullerenes was de-

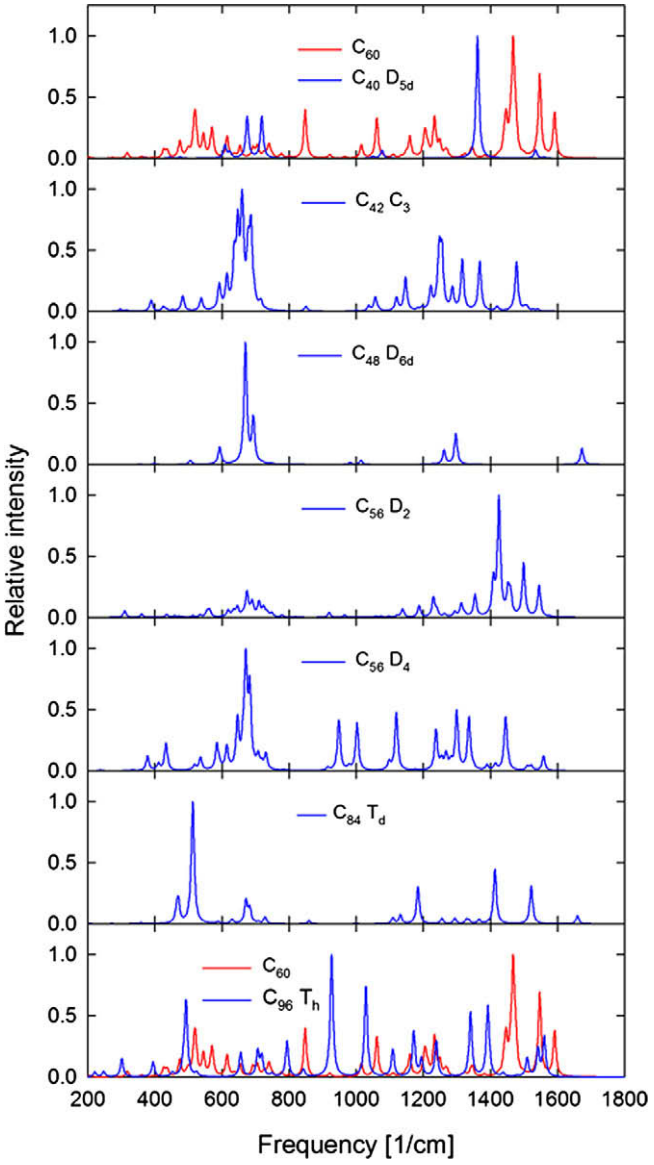

Fig. 5. IR spectra of the fullerenes in Table 2 yielded by DFT calculations with the PBE–PBE functional/6-31g basis set.

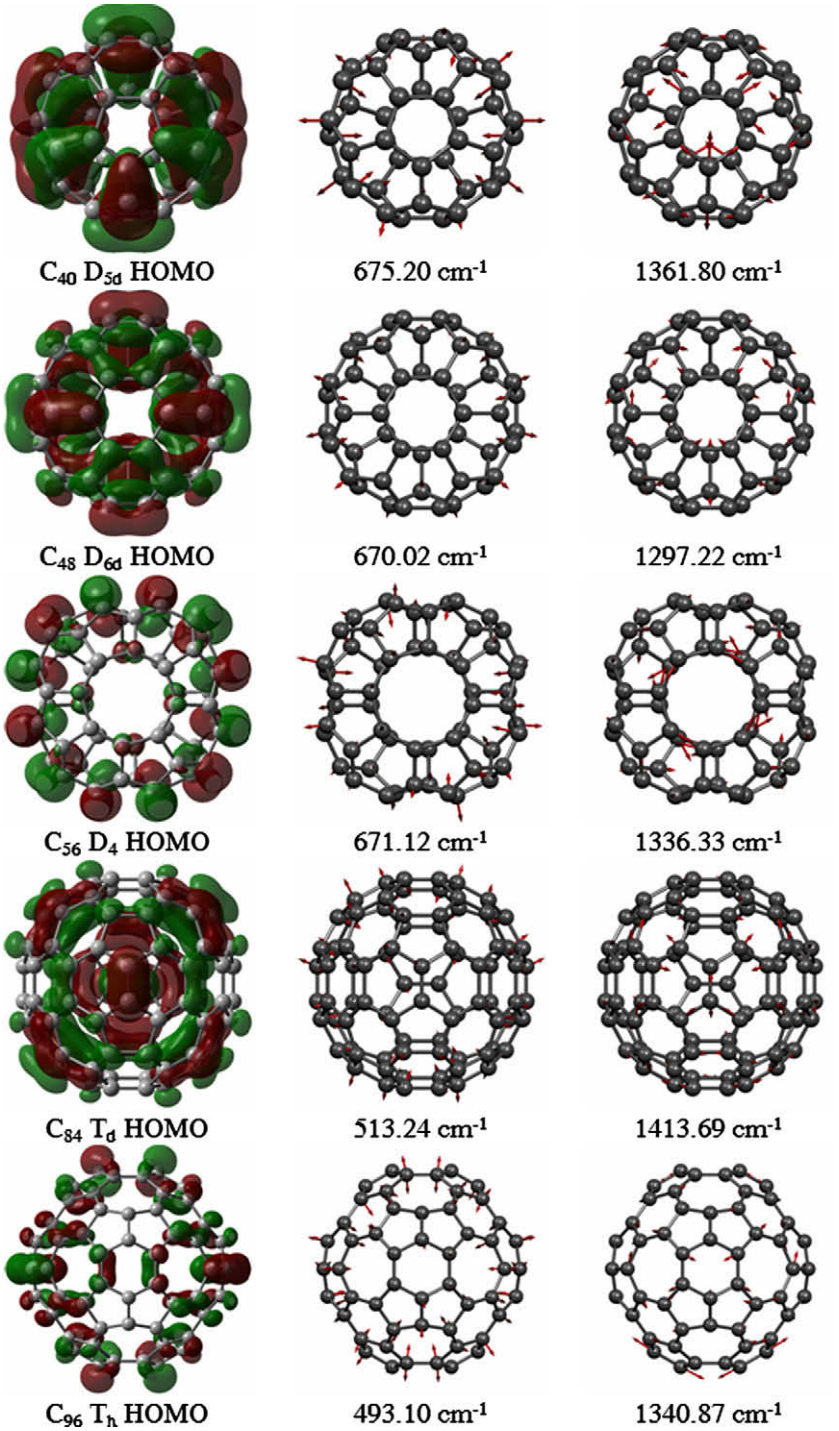

Fig. 6. Most intense IR-active vibrational modes of the fullerenes in Table 2.

signed and optimized at the PM3 level of theory; their aromaticity was evaluated, on these geometries, by the aid of the HOMA index [39–43]. However, the PM3 method is rather poor and belongs to history. Calculations at the more actual DFT methods are imposed. In order to adopt an appropriate exchange-correlation function, we compared the results obtained for the C_{60} fullerene with the widely used B3LYP function [46,47] and with the more recent function, PBE–PBE [48].

The PBE–PBE functional reproduces well the experimental HOMO–LUMO gap of C_{60} (1.6–1.85 eV.), giving 1.770 eV (1.668 eV) with the 6-31g (6-31g(d)) basis set, while the B3LYP function performs rather poorly, yielding 2.762 eV. Consequently, we have employed the PBE–PBE/6-31g combination in the production calculations.

As can be seen, the HOMO–LUMO gap decreases from C_{40} to C_{56} and interestingly, the gap for C_{84} is significantly larger than the rest of the investigated cages.

Among the simulated IR spectra, shown in Fig. 5, for comparison purposes, the spectrum of C_{60} was included in the top and bottom panels. Except for C_{56} (D_4), the structure of each spectrum is relatively simple, reflecting the high degree of symmetry of the cages. The spectra for C_{40}, C_{48}, and C_{84}, are remarkably simple and share

Table 4
Data of aromaticity: HOMA index in the whole molecule and selected flowers fws.

#	Structure	Sym.	HOMA	HOMA fws (entry)
1	C_{40}: 2[**5:6$_5$**]; 10R[5]	D_{5d}	−0.174	0.136
2	C_{42}: 2[**6:(5,6)$_3$**]; 3R[6]; 6R[5]	D_3	−0.043	**−0.016**
3	C_{48}: 2[**6:6$_6$**]; 12R[5]	D_{6d}	−0.633	**−0.193**
4	C_{56}: 2[**4:(7(5c))$_4$**]; 4R[6]; 8R[5]	D_4	−0.078	**0.001**
5	C_{56}: 2[**8:(5,6)$_4$**]; 4R[6]; 8R[5]	D_4	−0.310	**−0.348**
6	C_{64}: 2[4:(7(5*d*))$_4$]; 4R[6]; 4R[5]	D_{4d}	−0.564	**−0.611**
7	C_{42}: 2[**6:(5,6)$_3$**]; 6R[6]; 3R[4]	D_{3h}	−0.028	**0.005**
8	C_{48}: 2[**6:(5,7)$_3$**]; 12R[5]	D_{3d}	−0.076	**0.177**
9	C_{84}: 4[**6:(5,6)$_3$**]; 4[6:(0,6)$_3$]		0.286	**0.318**
	4[*6:6$_6$*]; 4[6:(0,5)$_3$]	T_d	–	*0.360*
10	C_{96}: 4[**6:(5,7)$_3$**]; 4[6:(0,5)$_3$]; 6R[6]	T_h	0.287	**0.335**
11	C_{60}: 4[**6:(5,6)$_3$**]; 4R[6]	I_h	0.261	**0.260**
12	[6] Coronene, [6:6$_6$]; (see entries 3, 9)	D_{6h}	0.715	−0.193 (3) 0.360 (9)
13	[6]Sumanene, [6:(5,6)$_3$]; (see entries 2, 7, 9, 11)	D_{3h}	−0.071	−0.016 (2) 0.005 (7) 0.318 (9) 0.260 (11)
14	[6]Corazene/isocoronene, [6:(5,7)$_3$]; (see entries 8, 10)	D_{3h}	0.594	0.177 (8) 0.335 (10)

the common feature of membership in point groups characterized by dihedral reflections (D_{5d}, D_{6d}, and T_d, respectively).

Almost all the molecules studied show one of their most intense peaks in the range 600–700 cm^{-1}. (C_{42}: 646.895, C_{56}, D_4: 671.119, C_{40}: 675.204, C_{48}: 670.017 cm^{-1}). These vibrations mainly arise from out-of-plane atomic motions and the atoms involved are located on the boundary of the flowers in question (Fig. 6). In the case of C_{84}, the low-frequency dominant normal mode is shifted towards even lower frequencies (513.2 cm^{-1}) due to the greater mass in the neighborhood of the flowers.

Other significant vibrations are located in the range 1250–1430 cm^{-1}. These types of vibrations characterize the atoms of flowers, and arise mainly from in-plane atomic motions. Fig. 6 shows the displacement patterns of the most intense IR-active modes.

The HOMO orbital is localized particularly on sumanenic faces, whereas the LUMO orbital is more delocalized. This could suggest a possible Jahn–Teller [49] modification or distortion of the structure. This structure has a semiconducting character if we consider the value of the HOMO–LUMO gap (3.159 eV); because both boundary orbitals are located in the negative domain of eigenvalues, the structure is a pseudo-closed cage and an electron acceptor.

In evaluation of the aromaticity (and stability) of the discussed fullerenes, some data, external to the fullerene cages were needed. Thus we calculated the HOMA index of the most frequently three flowers: coronene, sumanene and corasene, as hydrocarbon molecules; data are included in the bottom of Table 4. The corresponding last columns collect the values for these flowers within the discussed fullerenes.

Noticeable is the variation in aromaticity of one and the same flower function of the molecular context, when the strain plays an important destabilizing role and consequently will lower the HOMA values: (i) for Coronene (entry 12, Table 4), the value in the more relaxed #9 approaches that in the free hydrocarbon; (ii) for Sumanene (entry 13, Table 4), the maximum value is reached in #9 C_{84}, as expected for a disjoint flower Sumanene tessellation; (iii) for Corazene/iso-Coronene flower (entry 14, Table 4), the maximum value of HOMA is obtained for the cage #10, which shows the lowest strain (among the studied fullerenes) and a relatively low ratio HF/GAP (entry 10, the last two columns, Table 2). These data could encourage the chemist in finding routes for such, yet hypothetical, non-classical fullerenes.

4. Conclusions

Fullerenes tessellated by joint and disjoint circulenes/flowers, were shown to be relatively stable molecular structures and it is hoped that they can be obtained from currently available bowl-shaped precursors. The theoretical coverings were developed by sequential map operations, as implemented in our software program, CageVersatile.

Various quantum calculations and the HOMA index of aromaticity were used to evaluate the stability of the novel designed fullerenes.

DFT calculations using the basis set 6-31g and exchange-correlation functional PBE–PBE yield HOMO–LUMO gaps decreasing from C_{40} to C_{56}, the gap for C_{84} being however significantly larger than for the rest of the investigated cages. The structures of the calculated IR spectra are relatively simple, reflecting the high degree of symmetry of the cages considered. Almost all of the molecules studied have one of their most intense vibrations in the range 600–700 cm^{-1}, and this arises from out-of-plane atomic motions on the boundaries of the featured flowers. The other major IR-active vibrations located in the range 1250–1430 cm^{-1} arise mainly from in-plane atomic motions. The HOMO orbitals are localized particularly on flower faces and the more delocalized LUMO orbitals suggest possible Jahn–Teller distortions of the structures.

The variation in aromaticity of one and the same flower, function of the molecular context, can be explained by considering the strain of cages as an important destabilizing factor, which leads to lower HOMA values in comparison to those shown by these flowers calculated as hydrocarbon molecules.

Acknowledgments

The article is supported in part by the Romanian Grant ID_506/2007–2009 and by the Bilateral Project Romania–Slovenia, No. 26/2008.

References

[1] H.W. Kroto, J.R. Heath, S.C. O'Brien, R.F. Curl, R.E. Smalley, Nature 318 (1985) 162.
[2] W. Kraetschmer, L.D. Lamb, K. Fostiropoulos, D.R. Huffman, Nature 347 (1990) 354.
[3] H.W. Kroto, J.E. Fischer, D.E. Cox (Eds.), The Fullerenes, Pergamon, Oxford, 1993.

[4] H.W. Kroto, D.R.M. Walton (Eds.), The Fullerenes: New Horizons for the Chemistry Physics and Astrophysics of Carbon, Cambridge University Press, Cambridge, 1993.
[5] M. Endo, S. Iijima, M.S. Dresselhaus, Carbon Nanotubes, Pergamon, 1996.
[6] K. Tanaka, T. Yamabe, K. Fukui, The Science and Technology of Carbon Nanotubes, Elsevier, 1999.
[7] A.T. Balaban (Ed.), From Chemical Topology to Three-Dimensional Geometry, Plenum Press, New York, 1997.
[8] L.A. Paquette, D.W. Balogh, R. Usha, D. Koutz, G.G. Cristoph, Science 211 (1981) 575.
[9] K. Yamamoto, Pure Appl. Chem. 65 (1993) 157.
[10] H. Sakurai, T. Daiko, T. Hirao, Science 301 (2003) 1878.
[11] H. Sakurai, T. Daiko, H. Sakane, T. Amaya, T. Hirao, J. Am. Chem. Soc. 127 (2005) 11580.
[12] E. Clar, Polycyclic Hydrocarbons, Academic Press, London, 1964.
[13] E. Clar, The Aromatic Sextet, Wiley, New York, 1972.
[14] P.W. Fowler, T. Pisanski, J. Chem. Soc. Faraday Trans. 90 (1994) 2865.
[15] J.R. Dias, J. Chem. Inf. Comput. Sci. 39 (1999) 144.
[16] S.J. Cyvin, I. Gutman, Kekule Structures in Benzenoid Hydrocarbons, Lecture Notes in Chemistry, vol. 46, Springer-Verlag, Berlin, 1988.
[17] W.Ch. Shiu, P.Ch.B. Lam, H. Zhang, J. Mol. Struct. (THEOCHEM) 622 (2003) 239.
[18] X. Liu, D.J. Klein, T.G. Schmalz, Fullerene Sci. Technol. 2 (1994) 405.
[19] A.E. Vizitiu, Modeling Molecular Structures and Properties by the Aid of Topological Descriptors, Ph.D. Thesis, Cluj-Napoca, 2007.
[20] P. Fowler, D.E. Manolopoulos, An Atlas of Fullerenes, Clarendon Press, Oxford, 1995.
[21] R.C. Haddon, J. Am. Chem. Soc. 109 (1987) 1676.
[22] R.C. Haddon, J. Am. Chem. Soc. 120 (1998) 10494.
[23] G. Sun, M. Kertesz, J. Phys. Chem. A 105 (2001) 5212.
[24] M.V. Diudea, P.E. John, A. Graovac, M. Primorac, T. Pisanski, Croat. Chem. Acta 76 (2003) 153.
[25] M.V. Diudea, M. Ştefu, P.E. John, A. Graovac, Croat. Chem. Acta 79 (2006) 355.
[26] A.E. Vizitiu, M.V. Diudea, S. Nikolić, D. Janežić, J. Chem. Inf. Model. 46 (2006) 2574.
[27] M.V. Diudea, Cs.L. Nagy, Periodic Nanostructures, Springer, 2007.
[28] M.V. Diudea (Ed.), Nanostructures, Novel Architecture, Nova, 2005.
[29] M. Randić, Chem. Rev. 103 (2003) 3449.
[30] E. Clar, U. Sanigok, M. Zander, Tetrahedron 24 (1968) 2817.
[31] J.M. Schulman, R.L. Disch, J. Phys. Chem. A 101 (1997) 9176.
[32] T.A. Keith, R.F.W. Bader, Chem. Phys. Lett. 210 (1993) 223.
[33] P. Lazzeretti, in: J.W. Emsley, J. Feeney, L.H. Sutcliffe (Eds.), Current Progress in Nuclear Magnetic Resonance Spectroscopy, vol. 36, Elsevier, Amsterdam, 2000, pp. 1–88.
[34] A. Acocella, E.W.A. Havenith, E. Steiner, P.W. Fowler, L.W. Jenneskens, Chem. Phys. Lett. 363 (2002) 64.
[35] A. Ciesielski, M.K. Cyranski, T.M. Krygowski, P.W. Fowler, M. Lillington, J. Org. Chem. 71 (2006) 6840.
[36] M.V. Diudea, Forma (Tokyo) 19 (2004) 131.
[37] M. Stefu, M.V. Diudea, CageVersatile 1.3, Babes-Bolyai University, Cluj-Napoca, 2003.
[38] A.J. Stone, D.J. Wales, Chem. Phys. Lett. 128 (1986) 501.
[39] T.M. Krygowski, J. Chem. Inf. Comput. Sci. 33 (1993) 70.
[40] T.M. Krygowski, A. Ciesielski, C.W. Bird, A. Kotschy, J. Chem. Inf. Comput. Sci. 35 (1995) 203.
[41] T.M. Krygowski, A. Ciesielski, J. Chem. Inf. Comput. Sci. 35 (1995) 1001.
[42] T.M. Krygowski, M. Cyranski, A. Ciesielski, B. Swirska, P. Leszczynski, J. Chem. Inf. Comput. Sci. 36 (1996) 1135.
[43] T.M. Krygowski, M.K. Cyranski, Chem. Rev. 101 (2001) 1385.
[44] Cs.L. Nagy, M.V. Diudea, JSCHEM Software, Babes-Bolyai University, 2008.
[45] M.J. Frisch, G.W. Trucks, H.B. Schlegel, G.E. Scuseria, M.A. Robb, J.R. Cheeseman, J.A. Montgomery Jr., T. Vreven, K.N. Kudin, J.C. Burant, J.M. Millam, S.S. Iyengar, J. Tomasi, V. Barone, B. Mennucci, M. Cossi, G. Scalmani, N. Rega, G.A. Petersson, H. Nakatsuji, M. Hada, M. Ehara, K. Toyota, R. Fukuda, J. Hasegawa, M. Ishida, T. Nakajima, Y. Honda, O. Kitao, H. Nakai, M. Klene, X. Li, J.E. Knox, H.P. Hratchian, J.B. Cross, C. Adamo, J. Jaramillo, R. Gomperts, R.E. Stratmann, O. Yazyev, A.J. Austin, R. Cammi, C. Pomelli, J.W. Ochterski, P.Y. Ayala, K. Morokuma, G.A. Voth, P. Salvador, J.J. Dannenberg, V.G. Zakrzewski, S. Dapprich, A.D. Daniels, M.C. Strain, O. Farkas, D.K. Malick, A.D. Rabuck, K. Raghavachari, J.B. Foresman, J.V. Ortiz, Q. Cui, A.G. Baboul, S. Clifford, J. Cioslowski, B.B. Stefanov, G. Liu, A. Liashenko, P. Piskorz, I. Komaromi, R.L. Martin, D.J. Fox, T. Keith, M.A. Al-Laham, C.Y. Peng, A. Nanayakkara, M. Challacombe, P.M.W. Gill, B. Johnson, W. Chen, M.W. Wong, C. Gonzalez, J.A. Pople, Gaussian 03, Revision B.05, Gaussian, Inc., Pittsburgh, PA, 2003.
[46] A.D. Becke, J. Chem. Phys. 98 (1993) 5648.
[47] C. Lee, W. Yang, R.G. Parr, Phys. Rev. B 37 (1988) 785.
[48] J.P. Perdew, K. Burke, M. Ernzerhof, Phys. Rev. Lett. 77 (1996) 3865.
[49] H.A. Jahn, E. Teller, Proc. R. Soc. (London) A161 (1937) 220.